

---

# Hamiltonian Monte Carlo Acceleration Using Neural Network Surrogate functions

---

**Cheng Zhang**

Department of Mathematics  
University of California, Irvine  
Irvine, CA 92697  
chengz4@uci.edu

**Babak Shahbaba**

Department of Statistics  
University of California, Irvine  
Irvine, CA 92697  
babaks@uci.edu

**Hongkai Zhao**

Department of Mathematics  
University of California, Irvine  
Irvine, CA 92697  
zhao@math.uci.edu

## Abstract

Relatively high computational cost for Bayesian methods often limits their application for big data analysis. In recent years, there have been many attempts to improve computational efficiency of Bayesian inference. Here we propose an efficient and scalable computational technique for a state-of-the-art Markov Chain Monte Carlo (MCMC) methods, namely, Hamiltonian Monte Carlo (HMC). The key idea is to explore and exploit the regularity in parameter space for the underlying probabilistic model to construct an effective approximation of the collective geometric and statistical properties of the whole observed data. To this end, we use shallow neural networks along with efficient learning algorithms. The choice of basis functions (or hidden units in neural networks) and the optimized learning process provides a flexible, scalable and efficient sampling algorithm. Experiments based on simulated and real data show that our approach leads to substantially more efficient sampling algorithms compared to existing state-of-the art methods.

## 1 Introduction

Bayesian statistics has provided a principled and robust framework to create many important and powerful data analysis methods over the past several decades. Given a probabilistic model for the underlying mechanism of observed data, Bayesian methods properly quantify uncertainty and reveal the landscape or global structure of the parameter space. However, these methods tend to be computationally intensive since Bayesian inference usually requires the use of MCMC algorithms to simulate samples from intractable distributions. Although the simple Metropolis algorithm [1] is often effective at exploring low-dimensional distributions, it can be very inefficient for complex, high-dimensional distributions: successive states may exhibit high autocorrelation, due to the random walk nature of the movement. As a result, the effective sam-

ple size tends to be quite low and the convergence to the true distribution is very slow. Hamiltonian Monte Carlo (HMC) [3, 4] reduces the random walk behavior of Metropolis by Hamiltonian dynamics, which uses gradient information to propose states that are distant from the current state, but nevertheless have a high probability of acceptance.

Although HMC explores the parameter space more efficiently than random walk Metropolis does, it does not fully exploit the structure (i.e., geometric properties) of parameter space [5] since dynamics are defined over Euclidean space. To address this issue, Girolami and Calderhead [5] proposed a new method, called Riemannian Manifold HMC (RMHMC), that uses the Riemannian geometry of the parameter space [6] to improve standard HMC's efficiency by automatically adapting to local structures.

To make such geometrically motivated methods practical for big data analysis, one needs to combine them with efficient and scalable computational techniques. A common bottleneck for using such sampling algorithms for big data analysis is repetitive evaluations of functions, their derivatives, geometric and statistical quantities that involves the whole observed data and maybe a complicated model. A natural question is how to construct effective approximation of these quantities that provides a good balance between accuracy and computation cost. One common approach is subsampling (see, for example, [7, 8, 9, 10]), which restricts the computation to a subset of the observed data. This is based on the idea that big datasets contain a large amount of redundancy so the overall information can be retrieved from a small subset. However, in general applications, we cannot simply use random subsets for this purpose: the amount of information we lose as a result of random sampling leads to non-ignorable loss of accuracy, which in turn has a substantial negative impact on computational efficiency [11]. Therefore, in practice, it is a challenge to find good criteria and strategies for an appropriate and effective subsampling.

Another approach is to exploit smoothness or regularity in parameter space, which is true for most statistical models. This way, one could find computationally cheaper surrogate functions to substitute the expensive target (or potential energy) functions [14, 15, 16]. However, the usefulness of these methods is often limited to moderate dimensional problems because of the cost of inference or precomputing scale needed to achieve desired approximation accuracy.

In this work we propose to use shallow neural networks and efficient learning algorithms to construct an effective approximation of the collective geometric and statistical properties of the whole observed data. The randomly oriented and positioned basis functions (or hidden units in neural networks) combined with the optimized learning process can incorporate correct criteria for an efficient implicit subsampling resulting in both flexible and scalable approximation. Our proposed method provides a natural framework to incorporate surrogate functions in the sampling algorithms such as HMC, and it can be easily extended to geometrically motivated methods such as Riemannian Manifold HMC.

Our paper is organized as follows. An overview of HMC and RMHMC is given in Section 2. Our neural network surrogate HMC is explained in detail in Section 3. Experiment results on simulated and real data are presented in Section 4. Finally, Section 5 is devoted to discussion and future work.

## 2 Preliminaries

### 2.1 Hamiltonian Monte Carlo

In Bayesian Statistics, we are interested in sampling from the posterior distribution of the model parameters  $q$  given the observed data,  $Y = (y_1, y_2, \dots, y_N)^T$ ,

$$P(q|Y) \propto \exp(-U(q)), \tag{1}$$

where the potential energy function  $U$  is defined as

$$U(q) = -\sum_{i=1}^N \log P(y_i|q) - \log P(q). \quad (2)$$

The posterior distribution is almost always analytically intractable. Therefore, MCMC algorithms are typically used for sampling from the posterior distribution to perform statistical inference. As the number of parameters increases, however, simple methods such as random walk Metropolis [1] and Gibbs sampling [2] may require a long time to converge to the target distribution. Moreover, their explorations of parameter space become slow due to inefficient random walk proposal-generating mechanisms, especially when there exist strong dependencies between parameters in the target distribution. By inclusion of geometric information from the target distribution, HMC [3, 4] introduces a Hamiltonian dynamics system with auxiliary momentum variables  $p$  to propose samples of  $q$  in a Metropolis framework that explores the parameter space more efficiently compared to standard random walk proposals. More specifically, HMC generates proposals jointly for  $q$  and  $p$  using the following system of differential equations:

$$\frac{dq_i}{dt} = \frac{\partial H}{\partial p_i} \quad (3)$$

$$\frac{dp_i}{dt} = -\frac{\partial H}{\partial q_i} \quad (4)$$

where the Hamiltonian function is defined as  $H(q, p) = U(q) + \frac{1}{2}p^T M^{-1}p$ . The quadratic kinetic energy function  $K(p) = \frac{1}{2}p^T M^{-1}p$  corresponds to the negative log-density of a zero-mean multivariate Gaussian distribution with the covariance  $M$ . Here,  $M$  is known as the mass matrix, which is often set to the identity matrix,  $I$ , but can be used to precondition the sampler using Fisher information [5]. Starting from the current state  $(q, p)$ , the Hamiltonian dynamics system (3),(4) is simulated for  $L$  steps using the leapfrog method, with a stepsize of  $\epsilon$ . The proposed state,  $(q^*, p^*)$ , which is at the end of the trajectory, is accepted with probability  $\min(1, \exp[-H(q^*, p^*) + H(q, p)])$ . By simulating the Hamiltonian dynamics system together with the correction step, HMC generates samples from a joint distribution

$$P(q, p) \propto \exp\left(-U(q) - \frac{1}{2}p^T M^{-1}p\right)$$

Notice that  $q$  and  $p$  are separated, the marginal distribution of  $q$  then follows the target distribution. These steps are presented in Algorithm 1. Following the dynamics of the assumed Hamiltonian system, HMC can generate distant proposals (i.e., low autocorrelation) with high acceptance probability (i.e., conservation of Hamiltonian) which allows an efficient exploration of parameter space.

## 2.2 Riemannian Manifold HMC

Although HMC explores the target distribution more efficiently than random walk Metropolis, it does not fully exploit the geometric structures of the underlying probabilistic model since a flat metric (i.e.,  $M = I$ ) is used. Using more geometrically motivated methods could substantially improve sampling algorithms' efficiency. Recently, Girolami and Calderhead [5] proposed a new method, called Riemannian Manifold HMC (RMHMC), that exploits the Riemannian geometry of the target distribution to improve standard HMC's efficiency by automatically adapting to local structures. To this end, instead of the identity mass matrix commonly used in standard HMC, they use a position-specific mass matrix  $M = G(q)$ . More specifically, they set  $G(q)$  to the Fisher information matrix, and define Hamiltonian as follows:

$$H(q, p) = U(q) + \frac{1}{2} \log \det G(q) + \frac{1}{2} p^T G(q)^{-1} p = \phi(q) + \frac{1}{2} p^T G(q)^{-1} p \quad (5)$$

---

**Algorithm 1: Hamiltonian Monte Carlo**

---

**Input:** Starting position  $q^{(1)}$  and step size  $\epsilon$

```
for  $t = 1, 2, \dots$  do
  Resample momentum  $p$ 
   $p^{(t)} \sim \mathcal{N}(0, M)$ ,  $(q_0, p_0) = (q^{(t)}, p^{(t)})$ 
  Simulate discretization of Hamiltonian dynamics:
  for  $l = 1$  to  $L$  do
     $p_{l-1} \leftarrow p_{l-1} - \frac{\epsilon}{2} \frac{\partial U}{\partial q}(q_{l-1})$ 
     $q_l \leftarrow q_{l-1} + \epsilon M^{-1} p_{l-1}$ 
     $p_l \leftarrow p_l - \frac{\epsilon}{2} \frac{\partial U}{\partial q}(q_l)$ 
   $(q^*, p^*) = (q_L, p_L)$ 
  Metropolis-Hasting correction:
   $u \sim \text{Uniform}[0, 1]$ 
   $\rho = \exp[H(q^{(t)}, p^{(t)}) - H(q^*, p^*)]$ 
  if  $u < \min(1, \rho)$ , then  $q^{(t+1)} = q^*$ 
```

---

where  $\phi(q) := U(q) + \frac{1}{2} \log \det G(q)$ . Note that standard HMC is a special case of RMHMC with  $G(q) = I$ . Based on this dynamic, they propose the following HMC on Riemmanian manifold:

$$\begin{aligned} \dot{q} &= \nabla_p H(q, p) = G(q)^{-1} p \\ \dot{p} &= -\nabla_q H(q, p) = -\nabla_q \phi(q) + \frac{1}{2} \nu(q, p) \end{aligned} \quad (6)$$

With the shorthand notation  $\partial_i = \partial/\partial q_i$  for partial derivative, the  $i$ th element of the vector  $\nu(q, p)$  is

$$(\nu(q, p))_i = -p^T \partial_i (G(q)^{-1}) p = (G(q)^{-1} p)^T \partial_i G(q) G(q)^{-1} p$$

The above dynamic is non-separable (it contains products of  $q$  and  $p$ ), and the resulting proposal generating mechanism based on the standard leapfrog method is neither time-reversible nor symplectic. Therefore, the standard leapfrog algorithm cannot be used for the above dynamic [5]. Instead, we can use the Stömer-Verlet [12] method, known as generalized leapfrog [13],

$$p^{(t+1/2)} = p^{(t)} - \frac{\epsilon}{2} \left[ \nabla_q \phi(q^{(t)}) - \frac{1}{2} \nu(q^{(t)}, p^{(t+1/2)}) \right] \quad (7)$$

$$q^{(t+1)} = q^{(t)} + \frac{\epsilon}{2} \left[ G^{-1}(q^{(t)}) + G^{-1}(q^{(t+1)}) \right] p^{(t+1/2)} \quad (8)$$

$$p^{(t+1)} = p^{(t+1/2)} - \frac{\epsilon}{2} \left[ \nabla_q \phi(q^{(t+1)}) - \frac{1}{2} \nu(q^{(t+1)}, p^{(t+1/2)}) \right] \quad (9)$$

The resulting map is 1) deterministic, 2) reversible, and 3) volume-preserving. However, it requires solving two computationally intensive implicit equations (Equations (7) and (8)) at each leapfrog step.

### 3 Neural Network Surrogate HMC (NNS-HMC)

For HMC, the designed Hamiltonian dynamics contains the information from the target distribution through the potential energy  $U$  and its gradient. For RMHMC, more geometric structure (i.e., the Fisher information) is included through the mass matrix for kinetic energy. It is the inclusion of these information in the Hamiltonian dynamics that allows HMC and RMHMC to improve upon random walk Metropolis. However, one

common computational bottleneck for HMC and other Bayesian models for big data is repetitive evaluations of functions, their derivatives, geometric and statistical quantities. Typically, each evaluation involves the whole observed data. For example, one has to compute the potential  $U$  and its gradient from the equation (2) for HMC and mass matrix  $M$  and its inverse for RMHMC *at every time step*. When  $N$  is large, this can be extremely expensive to compute in real applications. In some problems, each evaluation may involve solving a computationally expensive problem. (See the inverse problem and Remark in Section 4.2.)

To alleviate this issue, in recent years several methods have been proposed to construct *surrogate* Hamiltonians. For relatively low dimensional spaces, (sparse) grid based piecewise interpolative approximation using precomputing strategy was developed in [15]. Such grid based methods are difficult to extend to high dimensional spaces due to the use of structured grids. Alternatively, we can use Gaussian process model, which are commonly used as surrogate models for emulating expensive-to-evaluate functions, to learn the target functions from early evaluations (training data) [14, 16, 17]. However, Gaussian process models are often limited by the sizes of the training set because of the computation cost associated with inverting the covariance matrix. This is especially crucial in high dimensional spaces, where we need large training sets in order to achieve a reasonable level of accuracy.

Here we propose to use neural networks and efficient training algorithms to construct surrogate functions. Neural networks are capable of approximating any measurable function to any desired degree of accuracy [18]. Using neural networks and learning algorithms can incorporate desired criteria for an effective implicit subsampling. The choice of hidden units (basis functions) and the optimized learning process can be easily adapted to be problem specific and scalable. Moreover, instead of being limited by the sizes of training data, their generalization performance can be boosted as the number of training points increases. The computation complexity for a neural network is determined by the depth of the hidden layers and the numbers of hidden units for each layer. With appropriate training data, it can be expected that shallow neural networks with a few number of hidden units (at most several thousands) are sufficient to approximate smooth functions in high dimensional spaces well enough. Therefore, surrogate function provided by neural network approximations could be efficient even in high dimensional spaces.

### 3.1 Shallow neural network architecture

A typical shallow neural network architecture (i.e., a single-hidden layer feedforward scalar-output neural network) with  $s$  hidden units, a nonlinear activation function  $\sigma$ , and a scalar (for simplicity) output  $z$  for a given  $d$ -dimensional input  $q$  is defined as below

$$z(q) = \sum_{i=1}^s v_i \sigma(\mathbf{w}_i \cdot q + d_i) + b \quad (10)$$

where  $\mathbf{w}_i = [w_{i1}, w_{i2}, \dots, w_{id}]^T$  is the input weight vector for the  $i$ th hidden unit,  $v_i$  is the output weight for the  $i$ th hidden unit,  $d_i$  is the bias for the  $i$ th hidden unit, and  $b$  is the output bias. Given a training data set

$$\mathcal{T} = \{(q^{(j)}, t^{(j)}) | q^{(j)} \in \mathbb{R}^d, t^{(j)} \in \mathbb{R}, j = 1, \dots, N\}$$

the neural network can be trained by finding the optimal weights and biases  $\mathbf{W}$ ,  $\mathbf{v}$ ,  $\mathbf{d}$ ,  $b$  to minimize the cost,

$$C(\mathbf{W}, \mathbf{v}, \mathbf{d}, b) = \sum_{j=1}^N \|z(q^{(j)}) - t^{(j)}\|^2$$

### 3.2 Neural Network Approximation

Now, suppose that we have found an appropriate training data set (the early evaluations of HMC, for example). We need to find suitable learning algorithms to train our simple neural network efficiently. For a single-

---

**Algorithm 2: Extreme Learning Machine**

---

Given a training set  $\mathcal{T} = \{(I_j, t_j) | I_j \in \mathbb{R}^m, t_j \in \mathbb{R}^m, j = 1, \dots, N\}$ , activation function  $\sigma(x)$  and hidden node number  $s$

Step 1: Randomly assign input weight  $w_i$  and bias  $d_i, i = 1, \dots, s$

Step 2: Calculate the hidden layer output matrix  $H$

$$H_{ji} = \sigma(w_i I_j + d_i), \quad i = 1, \dots, s, j = 1, \dots, N$$

Step 3: Calculate the output weight  $v$

$$v = H^\dagger T, \quad T = [t_1, t_2, \dots, t_N]^T$$

where  $H^\dagger$  is the *Moore-Penrose generalized inverse* of matrix  $H$

---

hidden layer neural network, the most straightforward approach is to use the standard back-propagation algorithm [19]. However, as a gradient descent-based iterative algorithm, back-propagation is usually quite slow and can be trapped at some local minimum since the cost function is nonlinear, and for most cases, non-convex. An alternative approach could be the algebraic training methods [20, 21]. The key feature of algebraic training is that it decomposes the full optimization problem into multiple subproblems. By fixing some of the parameters, each subproblem can be solved very efficiently using simple linear algebra (e.g., solving a least square problem). Depending on the design objective, algebraic training can achieve exact or approximate matching of the data at the training points. Compared to the gradient descent-based techniques, algebraic training methods have reduced computational complexity and better generalization properties. A typical algebraic approach for single-hidden layer feedforward neural networks is extreme learning machine (ELM) [21], which is summarized in Algorithm 2. By fixing the input weights and biases (also known as 1.5-layer neural network), ELM solves the output weight by finding the smallest norm least square solution to the resulting linear equations system  $Hv = T$ .

### 3.3 Using Neural Network Surrogate Function

As mentioned in the previous sections, repetitive computation of Hamiltonian, its gradient and other quantities that involve all data set undermine the overall exploration efficiency for HMC. To alleviate this issue, we exploit the smoothness or regularity in parameter space, which is true for most statistical models. In particular, one can approximate target functions (e.g., the potential energy) using previous evaluations, which are usually discarded during the burn-in period of MCMC algorithms. Then, the resulting approximation can be used as a surrogate function to improve computational efficiency of sampling algorithms. To this end, the early evaluations during the MCMC run will be collected as a training set based on which we train a shallow neural network using fast algebraic approaches, such as ELM (Algorithm 2). The gradient of the scalar output  $z$  (see 10) for the neural network then can be computed as

$$\frac{\partial z}{\partial q} = \sum_{i=1}^s v_i \sigma'(\mathbf{w}_i \cdot q + d_i) \mathbf{w}_i \quad (11)$$

The choice of activation function is important to the approximation quality of our shallow neural network. Since the potential energy function in (2) is defined as the negative loglikelihood function,  $U(q) \rightarrow \infty$  as  $q$  moves away from the high density domain. To capture this feature of the target function, we choose the *softplus* function as our activation function (see Figure 1 for an example)

$$\sigma(x) = \log(1 + \exp(x))$$

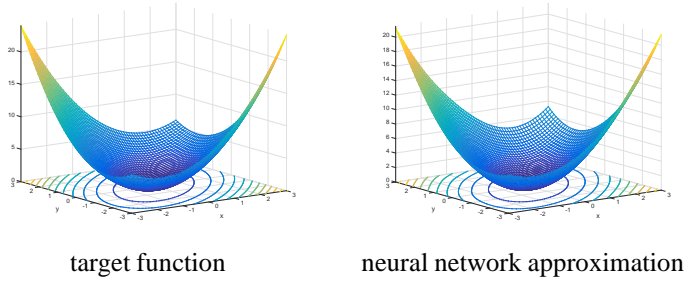


Figure 1: The neural network approximation using *softplus* activation function; target function  $f(x, y) = (x + y)^2/2 + 2(x - y)^2/3$  shown on the left panel is the negative loglikelihood function for a Gaussian distribution model  $Y \sim \mathcal{N}(\beta, [5/3, -1; -1, 5/3]^{-1})$  with a single data point  $\mathbf{0}$ . A single-hidden layer feedforward neural network with  $s = 20$  hidden units are trained based on 40 training data points sampled from the posterior distribution  $\mathcal{N}(\mathbf{0}, [5/3, -1; -1, 5/3]^{-1})$ .

From a function approximation point of view, a set of randomly assigned input weights and biases composed linearly inside the nonlinear activation function,  $\sigma(\mathbf{w}_i \cdot \mathbf{q} + d_i)$ , can be viewed as a set of basis functions shaped by  $\sigma$ , whose level sets are hyperplanes orientated by  $\mathbf{w}_i$  and shifted by  $d_i$  respectively. We use linear combination of this set of basis functions to approximate a smooth function in the parameter space using training set. An important property of this formulation is its scalability for any dimensions.

Following [14], we propose to run our method, henceforth called neural network surrogate Hamiltonian Monte Carlo (NNS-HMC, see Algorithm 3), in two phases: exploration phase and exploitation phase. During the exploration phase, we initialize the training data set  $D$  with an empty set or some samples from the prior distribution of parameters. We then run the standard HMC algorithm for a while and collect information from the new states (i.e., accepted proposals). When we have explored the high density region in parameter space sufficiently well, a shallow neural network is trained based on the collected training set  $D$  to form a surrogate to the potential energy function. The surrogate function will be used to approximate the information needed for HMC simulations later in the exploitation phase. Our proposed method provides a natural framework to incorporate surrogate functions in HMC. Moreover, it can be easily extended to RMHMC. To this end, the Hessian matrix of the surrogate function can be used to construct a metric in parameter space. We refer to this extended version of our method as NNS-RMHMC.

## 4 Experiments

In this section, we use several experiments based on logistic regression models and inverse problem for elliptic partial differential equation (PDE) to compare our proposed NNS-HMC method and its variant NNS-RMHMC to standard HMC and RMHMC in terms of sampling efficiency defined as time-normalized effective sample size (ESS). Given  $B$  MCMC samples for each parameter,  $\text{ESS} = B[1 + 2\sum_{k=1}^K \gamma(k)]^{-1}$ , where  $\sum_{k=1}^K \gamma(k)$  is the sum of  $K$  monotone sample autocorrelations [23]. We use the minimum ESS over all parameters normalized by the CPU time,  $s$  (in seconds), as the overall measure of efficiency:  $\min(\text{ESS})/s$ . The corresponding step sizes and leapfrog steps for HMC and RMHMC are chosen to make them stable and effective (e.g., reasonably high acceptance probability). The same settings are used for their counterparts, NNS-HMC and NNS-RMHMC.

For all experiments, 5000 samples are generated after discarding the first 5000 iterations. The accepted proposals during the burn-in period after a short warming-up session (say, the first 1000 iterations) are used as a training set for a shallow neural network with  $s = 2000$  hidden units for the simulated logistic regression

---

**Algorithm 3: Neural Network Surrogate HMC**

---

**Input:** Starting position  $q^{(1)}$ , step size  $\epsilon$  and number of hidden units  $s$   
Initialize the training data set:  $D = \emptyset$  or several random samples from the prior

**for**  $t = 1, 2, \dots, B$  **do**

    Resample momentum  $p$

$p^{(t)} \sim \mathcal{N}(0, M)$ ,  $(q_0, p_0) = (q^{(t)}, p^{(t)})$

    Simulate discretization of Hamiltonian dynamics and propose  $(q^*, p^*)$

    Metropolis-Hasting correction:

$u \sim \text{Uniform}[0, 1]$ ,  $\rho = \exp[H(q^{(t)}, p^{(t)}) - H(q^*, p^*)]$

**if**  $u < \min(1, \rho)$ , **then**  $q^{(t+1)} = q^*$ ,  $D = D \cup \{(q^*, U(q^*))\}$

Train a neural network with  $s$  hidden units via ELM on  $D$  to form the surrogate function  $z$

**for**  $t = B + 1, B + 2, \dots$  **do**

    Resample momentum  $p$

$p^{(t)} \sim \mathcal{N}(0, M)$ ,  $(q_0, p_0) = (q^{(t)}, p^{(t)})$

    Simulate discretization of a new Hamiltonian dynamics using  $z$ :

**for**  $l = 1$  to  $L$  **do**

$p_{l-1} \leftarrow p_{l-1} - \frac{\epsilon}{2} \frac{\partial z}{\partial q}(q_{l-1})$

$q_l \leftarrow q_{l-1} + \epsilon M^{-1} p_{l-1}$

$p_l \leftarrow p_l - \frac{\epsilon}{2} \frac{\partial z}{\partial q}(q_l)$

$(q^*, p^*) = (q_L, p_L)$

    Metropolis-Hasting correction:

$u \sim \text{Uniform}[0, 1]$ ,  $\rho = \exp[H(q^{(t)}, p^{(t)}) - H(q^*, p^*)]$

**if**  $u < \min(1, \rho)$ , **then**  $q^{(t+1)} = q^*$

---

model with 50 parameters and  $s = 1000$  for the other lower dimension examples. The results are provided in Table 1. Our proposed methods substantially improve the efficiency of their counterparts by at least an order of magnitude.

#### 4.1 Logistic regression model

As our first example, we apply the above four methods (i.e., HMC, RMHMC, NNS-HMC, and NNS-RMHMC) to a simulation study based on a logistic regression model with 50 parameters and  $N = 10^5$  observations. The design matrix is  $X = (\frac{1}{10}\mathbf{1}, X_1)$  and true parameters  $\beta$  are uniformly sampled from  $[0, 1]^{50}$ , where  $X_1 \sim \mathcal{N}_{49}(\mathbf{0}, \frac{1}{100}I_{49})$ . The binary responses  $Y = (y_1, y_2, \dots, y_N)^T$  are sampled independently from Bernoulli distributions with probabilities  $p_i = 1/(1 + \exp(-x_i^T \beta))$ . We assume  $\beta \sim \mathcal{N}_{50}(\mathbf{0}, 100I_{50})$ , and sample from the corresponding posterior distribution.

Notice that the potential energy function  $U$  is now a convex function, the Hessian matrix is positive semi-definite everywhere. Therefore, we use the Hessian matrix of the surrogate as a local metric in NNS-RMHMC. For HMC, we set the step size and leapfrog steps  $\epsilon = 0.045$ ,  $L = 24$ . For RMHMC, we set the step size and leapfrog steps  $\epsilon = 0.54$ ,  $L = 2$ . Table 1 compares the performance of the algorithms. As we can see, NNS-HMC has substantially improved the sampling efficiency (by almost 30 times compared to HMC) in terms of time-normalized ESS. The one and two dimensional posterior marginals of some selected parameters given by HMC and NNS-HMC are also presented in the appendix, see Figure 2.

Next, we apply our method to two real datasets: Bank Marketing and Adult. The Bank Marketing dataset (40197 observations and 24 features) is collected based on direct marketing campaigns of a Portuguese banking institution aiming at predicting if a client will subscribe to a term deposit [25]. The Adult dataset (30560 observations and 27 features) has been used to determine whether a person makes over 50K a year.



Experiment	Method	AP	s/Iter	min(ESS)/s	Speed-up
LR (Simulation)	HMC	0.6656	$3.573E-01$	1.45	1
	RMHMC	0.8032	3.794	0.06	0.04
	NNS-HMC	0.6726	$1.364E-02$	37.83	<b>26.09</b>
	NNS-RMHMC	0.8162	$1.027E-01$	2.17	1.50
LR (Bank Marketing)	HMC	0.8038	$7.400E-02$	6.51	1
	RMHMC	0.9210	$6.305E-01$	0.56	0.08
	NNS-HMC	0.7944	$7.508E-03$	58.22	<b>8.94</b>
	NNS-RMHMC	0.9064	$2.741E-02$	14.41	2.21
LR (Adult Data)	HMC	0.8300	$7.898E-02$	0.21	1
	RMHMC	0.8526	$5.842E-01$	1.06	4.81
	NNS-HMC	0.8096	$9.914E-03$	2.66	12.09
	NNS-RMHMC	0.8400	$3.300E-02$	18.68	<b>84.90</b>
Elliptic PDE	HMC	0.7077	1.568	0.061	1
	RMHMC	0.8014	4.388	0.228	3.74
	NNS-HMC	0.7138	$7.419E-02$	1.410	23.11
	NNS-RMHMC	0.6584	$9.720E-02$	4.375	<b>71.72</b>

Table 1: Comparing the algorithms using logistic regression models and an elliptic PDE inverse problem. For each method, we provide the acceptance probability (AP), the CPU time (s) for each iteration and the time-normalized ESS.

Both datasets are available from the UCI Machine Learning Repository. All data sets are normalized to have mean zero and standard deviation one. The priors are the same as before. The trajectory lengths were set to 0.36 and 0.52 for Bank Marketing and Adult respectively. The results for the two data sets are summarized in Table 1. As before, both NNS-HMC and NNS-RMHMC improve their counterparts significantly.

## 4.2 Elliptic PDE inverse problem

Another computationally intensive model is the elliptic PDE inverse problem discussed in [24]. This classical inverse problem involves inference of the diffusion coefficient in an elliptic PDE which is usually used to model isothermal steady flow in porous media. Let  $c$  be the unknown diffusion coefficient and  $u$  be the pressure field, the forward model is governed by the elliptic PDE

$$\nabla_{\mathbf{x}} \cdot (c(\mathbf{x}, \theta) \nabla_{\mathbf{x}} u(\mathbf{x}, \theta)) = 0, \quad (12)$$

where  $\mathbf{x} = (x_1, x_2) \in [0, 1]^2$  is the spatial coordinate. The boundary conditions are

$$u(\mathbf{x}, \theta)|_{x_2=0} = x_1, \quad u(\mathbf{x}, \theta)|_{x_2=1} = 1 - x_1, \quad \frac{\partial u(\mathbf{x}, \theta)}{\partial x_1} \Big|_{x_1=0} = 0, \quad \frac{\partial u(\mathbf{x}, \theta)}{\partial x_1} \Big|_{x_1=1} = 0$$

A log-Gaussian process prior is used for  $c(\mathbf{x})$  with mean zero and an isotropic squared-exponential covariance kernel:

$$C(\mathbf{x}_1, \mathbf{x}_2) = \sigma^2 \exp\left(-\frac{\|\mathbf{x}_1 - \mathbf{x}_2\|_2^2}{2l^2}\right)$$

for which we set the variance  $\sigma^2 = 1$  and the length scale  $l = 0.2$ . Now, the diffusivity field can be easily parameterized with a Karhunen-Loeve (K-L) expansion:

$$c(\mathbf{x}, \theta) \approx \exp\left(\sum_{i=1}^d \theta_i \sqrt{\lambda_i} v_i(\mathbf{x})\right)$$

where  $\lambda_i$  and  $v_i(\mathbf{x})$  are the eigenvalues and eigenfunctions of the integral operator defined by the kernel  $C$ , and the parameter  $\theta_i$  are endowed with independent standard normal priors,  $\theta_i \sim \mathcal{N}(0, 0.5^2)$ , which

are the targets of inference. In particular, we truncate the K-L expansion at  $d = 20$  modes and condition the corresponding mode weights on data. Data are generated by adding independent Gaussian noise to observations of the solution field on a uniform  $11 \times 11$  grid covering the unit square.

$$y_j = u(\mathbf{x}_j, \theta) + \epsilon_j, \quad \epsilon_j \sim \mathcal{N}(0, 0.1^2), \quad j = 1, 2, \dots, N$$

The number of leap frog steps and step sizes are set to be  $L = 10$ ,  $\epsilon = 0.24$  for both HMC and NNS-HMC. Note that the potential energy function is no longer convex; therefore, we can not construct a local metric from the Hessian matrix directly. However, the diagonal elements

$$\frac{\partial^2 U}{\partial \theta_i^2} = \frac{1}{\sigma_\theta^2} + \sum_{j=1}^N \frac{1}{\sigma_y^2} \left( \frac{\partial u_j}{\partial \theta_i} \right)^2 - \sum_{j=1}^N \frac{\epsilon_j}{\sigma_y^2} \frac{\partial^2 u_j}{\partial \theta_i^2}, \quad \sigma_\theta = 0.5, \sigma_y = 0.1, \quad i = 1, 2, \dots, d$$

are highly likely to be positive in that the deterministic part (first two terms) is always positive and the noise part (last term) tends to cancel out. The diagonals of the Hessian matrix of surrogate therefore induce an effective local metric which can be used in NNS-RMHMC. A comparison of the results of all algorithms are presented in Table 1 and the one and two dimensional posterior marginals of some selected parameters given by HMC and NNS-HMC are attached in the appendix (see Figure 3). As before, NNS-HMC provides a substantial improvement in the sampling efficiency (more than 20 times). For the RMHMC methods, we set  $L = 3$ ,  $\epsilon = 0.8$ . As seen in the table, RMHMC is more efficient than HMC but still not as efficient as NNS-HMC. However, NNS-RMHMC improves RMHMC substantially and outperforms NNS-HMC. Although the metric induced by the diagonals of the Hessian matrix of surrogate may not be as effective as Fisher information, it is much cheaper to compute and provide a good approximation.

**Remark.** In addition to the usual computational bottleneck as in previous examples, e.g., large amount of data, there is another challenge on top of that for this example due to the complicated forward model. Instead of a simple explicit probabilistic model that prescribes the likelihood of data given the parameter of interest, a PDE (12) is involved in the probabilistic model. The evaluation of geometrical and statistical quantities, therefore, involves solving a PDE similar to (12) in each iteration of HMC and RHMHC. This is a preventive factor in practice. Using our methods based on neural network surrogates provide a huge advantage. Numerical experiments show a gain of efficiency by more than 20 times. Higher improvement is expected as the amount of data increases.

## 5 Discussion and Future Work

In this paper, we proposed an efficient and scalable computational model for Bayesian inference methods by exploring and exploiting regularity of probability models in parameter space. Our methods are based on training a shallow neural network surrogate after exploring the parameter space sufficiently well. However, waiting for the completion of the exploration phase in practice could be problematic when the mixing rate is low or the model is computationally demanding. Therefore, one of the future research directions could involve applying Markov chain regeneration technique to dynamically construct surrogate functions using all or part of the history of the Markov chain [26].

For HMC, gradient of the potential function is an important driving force in the Hamiltonian dynamics. Although accurate approximation of a well sampled smooth function automatically leads to accurate approximation of its gradient, this is not the case when the sampling is not well distributed. For example, when dense and well sampled training data sets are difficult to get in very high dimensions, one can incorporate the gradient information in the training process.

## References

- [1] N. Metropolis, A. W. Rosenbluth, M. N. Rosenbluth, A. H. Teller, and E. Teller. (1953) Equation of State Calculations by Fast Computing Machines. *The Journal of Chemical Physics*, **21**, pp. 1087–1092.
- [2] S. Geman and D. Geman. (1984) Stochastic relaxation, Gibbs distributions and the Bayesian restoration of images. *IEEE Transactions on Pattern Analysis and Machine Intelligence*, **6**: 721–741
- [3] S. Duane, A. D. Kennedy, B. J. Pendleton, and D. Roweth. (1987) Hybrid Monte Carlo. *Physics Letters B*, **195**, pp. 216 – 222.
- [4] R. M. Neal. (2011) MCMC using Hamiltonian dynamics, in *Handbook of Markov Chain Monte Carlo*, S. Brooks, A. Gelman, G. Jones, and X. L. Meng, eds., Chapman and Hall/CRC, pp. 113–162.
- [5] M. Girolami and B. Calderhead. (2011) Riemann manifold Langevin and Hamiltonian Monte Carlo methods. *Journal of the Royal Statistical Society, Series B, (with discussion)*, **73**, pp. 123–214.
- [6] S. Amari and H. Nagaoka. *Methods of Information Geometry*, volume 191 of Translations of Mathematical monographs, Oxford University Press, 2000.
- [7] M. Welling and Y.W. Teh. (2011) Bayesian learning via stochastic gradient langevin dynamics. In *Proceedings of the 28th International Conference on Machine Learning (ICML)*, pages 681–688.
- [8] M D. Hoffman, D. M. Blei, F. R. Bach. (2010) Online Learning for Latent Dirichlet Allocation. In *Neural Information Processing Systems (NIPS)*, pp. 856-864.
- [9] B. Shahbaba, S. Lan, W.O. Johnson, and R.M. Neal. (2014) Split Hamiltonian Monte Carlo. *Statistics and Computing*, **24**, pp. 339–349.
- [10] T. Chen, E. B. Fox, and C. Guestrin. (2014) Stochastic gradient Hamiltonian Monte Carlo. Preprint.
- [11] M.J. Betancourt. (2015) The Fundamental Incompatibility of Hamiltonian Monte Carlo and Data Subsampling, preprint: arXiv:1502.01510.
- [12] L. Verlet. (1967) Computer 'experiments' on classical fluids, I: Thermodynamical properties of Lennard-Jones molecules. *Phys. Rev*, **159**, pp. 98–103
- [13] B. Leimkuler and S. Reich. (2004) *Simulating Hamiltonian Dynamics*, Cambridge: Cambridge University Press.
- [14] C. E. Rasmussen. (2003) Gaussian processes to speed up hybrid monte carlo for expensive bayesian integrals. *Bayesian Statistics*, **7** pp. 651–659.
- [15] C. Anonymous (2015) Precomputing Strategy for Hamiltonian Monte Carlo Method Based on Regularity in Parameter Space. arXiv:1504.01418v1, Apr 2015. Unpublished manuscript.
- [16] S. Lan, T. Bui, M. Christie, A. Stuart, M. Girolami. (2015) Adaptive Geometric Monte Carlos Using Gaussian Process Emulation for Computation Extensive Models, *Technical Report*.
- [17] E. Meeds and M. Welling. (2014) GPS-ABC: Gaussian Process Surrogate Approximate Bayesian Computation. arXiv:1401.2838, January 2014. Unpublished manuscript.
- [18] K. Hornik, M. Stinchcombe and H. White. (1989) Multilayer feedforward networks are universal approximators. *Neural Networks*, **2**, pp. 349–358
- [19] D. E. Rumelhart, G. E. Hinton and R. J. Williams, (1986) Learning internal representations by error propagation. *Parallel Distributed Processing: Explorations in the Microstructure of Cognition*, **I**. Cambridge, MA: Bradford Books, pp. 318–362
- [20] S. Ferrari and R. F. Stengel. (2005) Smooth function approximation using neural networks. *IEEE Trans. Neural Networks*, **16**(1), pp. 24–38
- [21] G. B. Huang, Q. Y. Zhu and C. K. Siew. (2006) Extreme learning machine: Theory and applications. *Neurocomputing*, **70**(1-3), pp. 489–501
- [22] P. L. Bartlett. (1998) The Sample complexity of pattern classification with neural networks: the size of the weights is more important than the size of the network. *IEEE Trans. Inf. Theory*, **44**(2), pp. 525–536
- [23] C. J. Geyer. (1992) Practical Markov Chain Monte Carlo. *Statistical Science*, **7**, pp. 473–483.

- [24] P. R. Conard, Y. M. Marzouk, N. S. Pillai, and A. Smith. (2014) Asymptotically exact mcmc algorithms via local approximations of computationally intensive models, preprint arXiv:1402.1694v3, Nov 2014. Unpublished manuscript.
- [25] S. Moro, P. Cortez and P. Rita. (2014) A Data-Driven Approach to Predict the Success of Bank Telemarketing. *Decision Support Systems, Elsevier*, **62**, pp. 22–31.
- [26] W. R. Gilks, G. O. Roberts and S. K. Sahu. (1998) Adaptive Markov chain Monte Carlo through regeneration. *Journal of the American Statistical Association*, **93**, pp. 1045-1054.

## A Figures

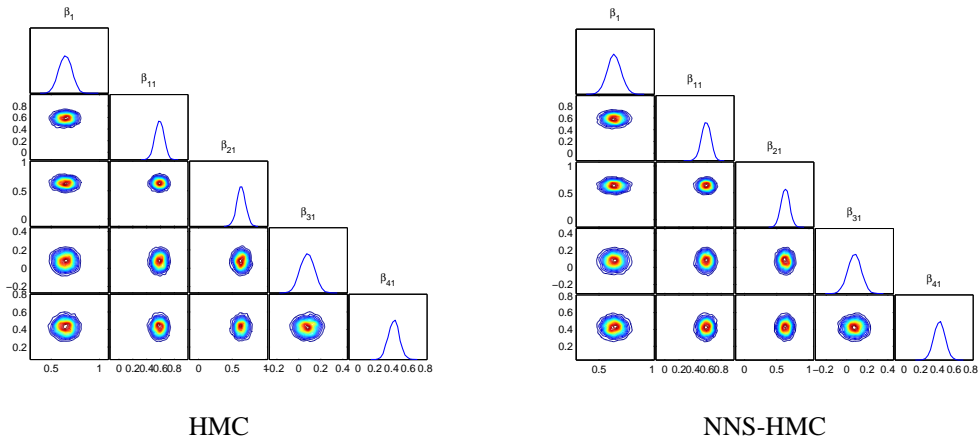


Figure 2: HMC vs NNSHMC: One- and two- dimensional posterior marginals of  $\beta_1, \beta_{11}, \beta_{21}, \beta_{31}, \beta_{41}$  in the simulated logistic regression model

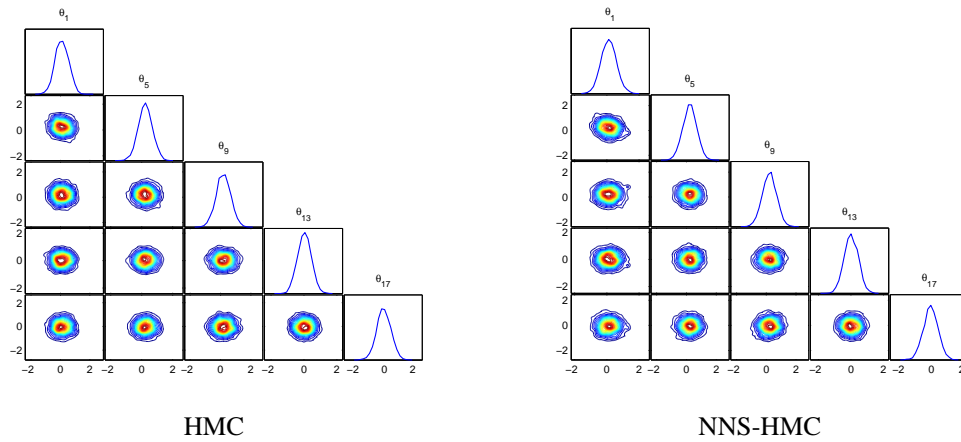


Figure 3: HMC vs NNSHMC: One- and two- dimensional posterior marginals of  $\theta_1, \theta_5, \theta_9, \theta_{13}, \theta_{17}$  in the elliptic PDE inverse problem